

Supporting Information

Tunneling across SAMs Containing Oligophenyl Groups

Carleen M. Bowers,^a Dmitrij Rappoport,^a Mostafa Baghbanzadeh,^a Felice C. Simeone,^a Kung-Ching Liao,^a Sergey N. Semenov,^a Tomasz Żaba,^b Piotr Cyganik,^b Alan Aspuru-Guzik,^a and George M. Whitesides^{a,c}*

^aDepartment of Chemistry and Chemical Biology, Harvard University,
12 Oxford Street, Cambridge, Massachusetts 02138 United States

^bSmoluchowski Institute of Physics, Jagiellonian University, ul. Lojasiewicza 11, 30-348
Krakow, Poland

^bKavli Institute for Bionano Science & Technology, Harvard University,
29 Oxford Street, Massachusetts 02138 United States

*Corresponding author, email: gwhitesides@gmwhgroup.harvard.edu

Experimental Details

Materials. Molecular precursors to all self-assembled monolayers (SAMs) were commercially available ($\geq 98\%$, Sigma-Aldrich) unless otherwise specified. All organic solvents were analytical grade (99%, Sigma-Aldrich) and were used as supplied. All compounds were stored under a nitrogen atmosphere at $< 4^\circ\text{C}$ to avoid degradation. To ensure that the compounds were free of contaminants, all stored compounds were examined by ^1H NMR prior to use.

Formation of SAMs of Oligophenylthiols (Ph_nSH) and -methanethiols ($\text{Ph}_n\text{CH}_2\text{SH}$), with $n = \text{number of Phenylene rings (} n = 1, 2, 3\text{)}$. We formed SAMs on template-stripped silver and gold substrate (Au^{TS} and Ag^{TS}).¹ Solutions of thiols (0.5-1mM) were made using anhydrous ethanol (200 proof); the solutions were purged with nitrogen before introduction of the metal substrate. HSPH is particularly sensitive to oxidation in solution; to minimize introduction of O_2 or H_2O from the surface of the metal substrate to the solution, we covered the substrate with anhydrous solvent before introduction to the thiol solution. The Au^{TS} and Ag^{TS} substrates were submerged in a 0.5-1mM ethanolic solution of thiolate for 16-24 hours at room temperature and under a nitrogen atmosphere. (The self-assembly of the aromatic thiols has to be performed in more dilute solutions than saturated n -alkanes due to poor solubility and possible multilayer formation). We rinsed the SAM-bound substrates with ethanol, and dried them under a gentle stream of nitrogen.

Formation of SAMs of Oligopolyphenylacetylenes ($\text{C}\equiv\text{CPh}_n$). We formed SAMs of $\text{C}\equiv\text{CPh}_n$ on template-stripped gold (Au^{TS}). Au^{TS} substrates were submerged in a 1mM solution of alkyne in anhydrous hexadecane for 48 hours at room temperature and under a nitrogen atmosphere. Due to the susceptibility of alkynes to oxidation in the presence of oxygen;² exposure of the substrate and solution to oxygen was minimized.³ We rinsed the SAM-bound

substrates with hexadecane, followed by ethanol, and dried them under a gentle stream of nitrogen.

Electrical measurements using Ga₂O₃/EGaIn top-electrodes. We used EGaIn (eutectic Ga-In; 74.5% Ga, 25.5% In) conical tips that were selected to be free of visible asperities (“selected tips”)⁴ on the surface of the Ga₂O₃. We measured charge-transport across the SAMs at ± 0.5 V by sweeping in both directions in steps of 0.05 V and starting at 0 V. Data for current density J (A/cm²) across SAMs of aromatic molecules exhibited a log-normal distribution; we fit Gaussian curves to histograms. We estimated the values of β (Å⁻¹) and J_0 (A/cm²) from linear regression analyses of the variation of values of $\langle \log|J| \rangle$ (Gaussian mean value of data for $\log|J|$) with the length d (Å) of the tunneling barrier, measured as the distance in Å between the anchoring atom and the distal H-atom of the molecules (Figure 1).

Table S1. Summary of static water-wetting contact angles (θ_s) for oligophenyl-acetylenes and -thiols on Au^{TS}. Results agree well with measurements previously reported.⁵⁻⁷

| Phenylacetylenes on Au ^{TS} | mean static contact angle (θ_s) and standard deviation | Phenylthiols on Au ^{TS} | Mean static contact angle (θ_s) and standard deviation |
|--------------------------------------|---|----------------------------------|---|
| C≡CPh ₁ | 82 ± 1 | SPh ₁ | 70 ± 2 |
| C≡CPh ₂ | 86 ± 2 | SPh ₂ | 75 ± 2 |
| C≡CPh ₃ | 82 ± 2 | SPh ₃ | 82 ± 2 |
| | | SCH ₂ Ph ₁ | 80 ± 2 |
| | | SCH ₂ Ph ₂ | 80 ± 2 |
| | | SCH ₂ Ph ₃ | 82 ± 2 |

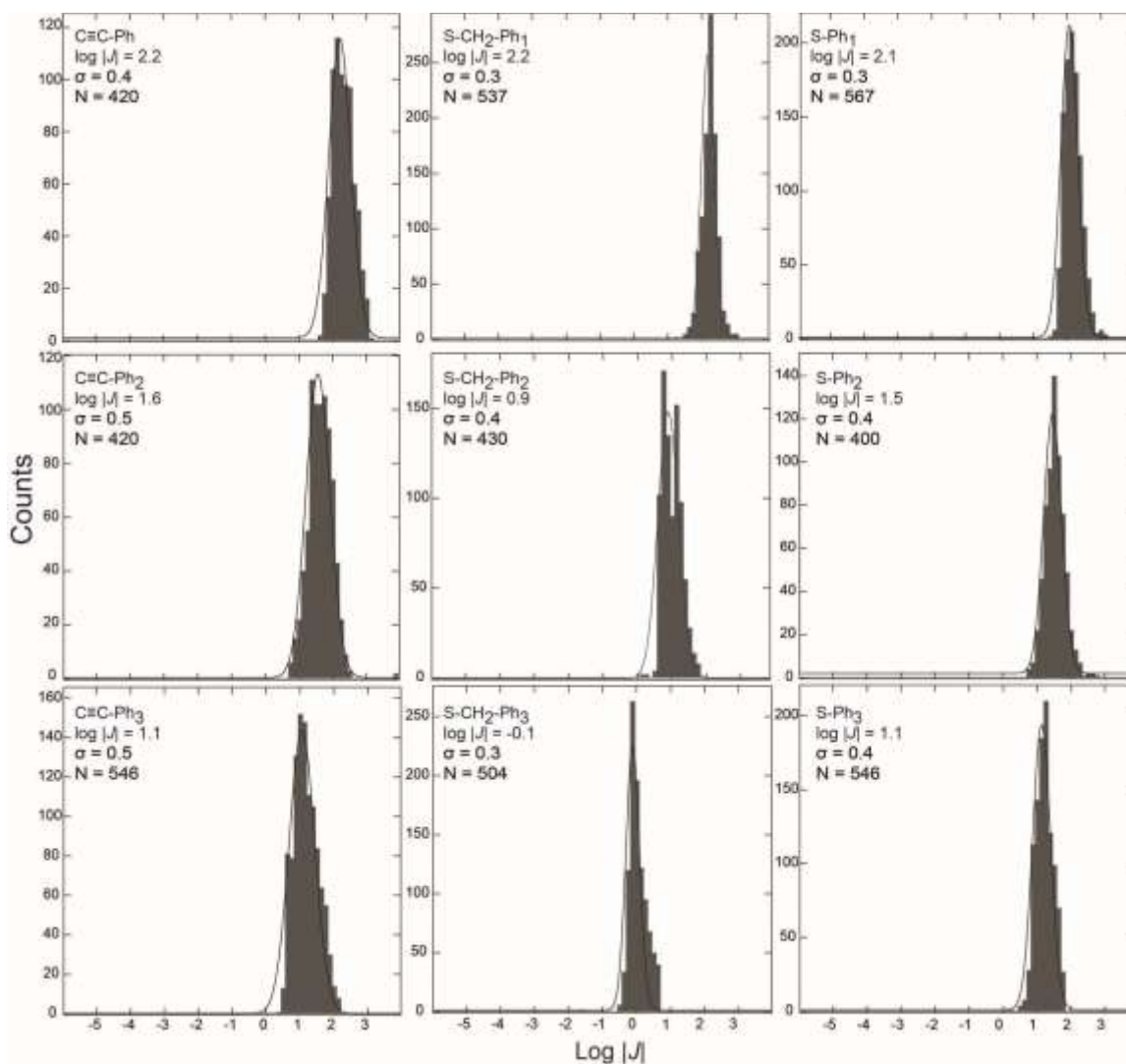


Figure S1. Histograms of $\log|J|$ at +0.5 V for across SAMs of oligophenyl-acetylenes (C≡CPh_n), -methanethiols (HSCH₂Ph_n), and -thiols (SPh_n) on Au^{TS} using selected conical tips that were free of visible surface asperities.³ Solid curves indicate a Gaussian fit, and N is the number of data points.

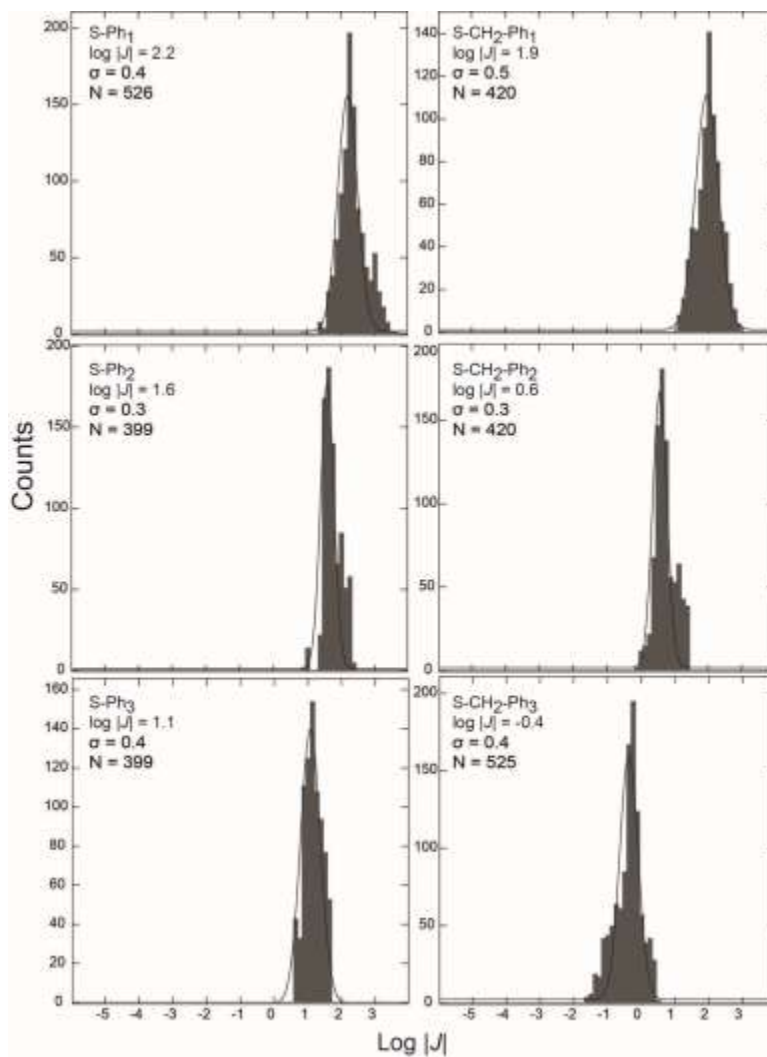


Figure S2. Histograms of $\log |J|$ at +0.5 V across SAMs of oligophenyl-thiols (SPh_n) and -methanethiols (HSCH₂Ph_n) on Ag^{TS} using “selected conical tips. Solid curves represent Gaussian fits, and N is the number of data points.

Table S2. Summary of the electrical measurements of tunneling across SAMs of oligophenylthiols (-SH), -methanethiols (-CH₂SH), and -acetylenes (-C≡CH). V = +0.5 V.

| SAM | Number of Junctions | Traces | $\langle \log J \rangle$ V=+0.5 V | σ_{\log} | |
|--|---------------------|--------|--|----------------------------|-------------|
| <i>Silver substrate</i> | | | | | |
| SPh | 25 | 525 | 2.2 | 0.4 | |
| SPh ₂ | 19 | 399 | 1.6 | 0.3 | |
| SPh ₃ | 19 | 399 | 1.1 | 0.4 | |
| | | | | Log J₀ | 2.9 ± 0.1 |
| | | | | β | 0.30 ± 0.02 |
| SCH ₂ Ph | 20 | 420 | 1.9 | 0.5 | |
| SCH ₂ Ph ₂ | 20 | 420 | 0.6 | 0.3 | |
| SCH ₂ Ph ₃ | 25 | 525 | -0.4 | 0.5 | |
| | | | | Log J₀ | 3.7 ± 0.3 |
| | | | | β | 0.66 ± 0.06 |
| S(CH ₂) _n CH ₃ | | | | Log J₀ | 3.6 ± 0.3 |
| | | | | β | 0.72 ± 0.05 |
| <i>Gold substrate</i> | | | | | |
| SPh | 27 | 567 | 2.1 | 0.3 | |
| SPh ₂ | 19 | 399 | 1.5 | 0.4 | |
| SPh ₃ | 26 | 546 | 1.1 | 0.4 | |
| | | | | Log J₀ | 2.7 ± 0.1 |
| | | | | β | 0.28 ± 0.03 |
| SCH ₂ Ph | 26 | 537 | 2.2 | 0.3 | |
| SCH ₂ Ph ₂ | 24 | 430 | 0.9 | 0.4 | |
| SCH ₂ Ph ₃ | 24 | 504 | -0.1 | 0.3 | |
| | | | | Log J₀ | 4.0 ± 0.3 |
| | | | | β | 0.66 ± 0.06 |
| C≡CPh | 20 | 420 | 2.2 | 0.4 | |
| C≡CPh ₂ | 20 | 420 | 1.6 | 0.5 | |
| C≡CPh ₃ | 26 | 546 | 1.1 | 0.5 | |
| | | | | Log J₀ | 3.0 ± 0.1 |
| | | | | β | 0.30 ± 0.02 |
| S(CH ₂) _n CH ₃ | | | | Log J₀ | 4.2 ± 0.2 |
| | | | | β | 0.76 ± 0.03 |

Computational details. We performed density functional theory (DFT) calculations on cluster models of gold and silver-bound compounds of oligophenyls using the B3LYP hybrid exchange-correlation functional⁸ and the resolution-of-the-identity approximation for the Coulomb interaction.⁹ We employed split-valence plus polarization basis sets,¹⁰ along with the corresponding auxiliary basis sets,¹¹ and small-core relativistic effective core potentials for Ag and Au¹² throughout. We carried out unrestricted structure optimizations on individual polyaromatic molecules attached to the Ag₉ and Au₁₀ metal clusters. We analyzed subsequently the orbital energies and orbital shapes of the molecular orbitals (MOs) of the metal–molecule complexes at their respective optimized structures. All computations used the Turbomole quantum chemical program suite.¹³ Spin-up (alpha) and spin-down (beta) MOs are shown separately.

Table S3. Orbital energies (eV) and shapes of the high-lying MOs localized on the C≡C bond for the Au/C≡CPh_n Series.

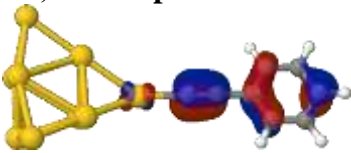
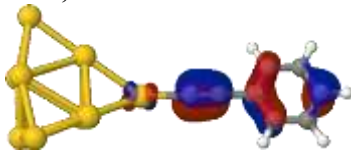
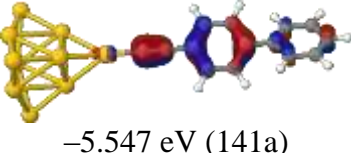
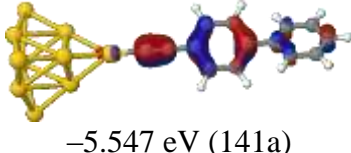
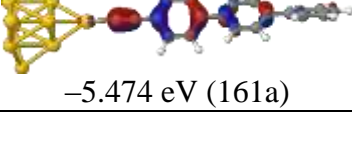
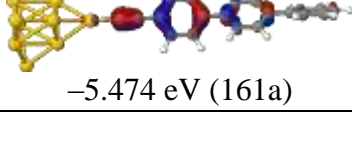
| Cluster | MO, C≡C alpha | MO, C≡C beta |
|-------------------------------------|---|--|
| PhC≡CAu ₁₀ |  -5.723 eV (121a) |  -5.724 eV (121a) |
| Ph ₂ C≡CAu ₁₀ |  -5.547 eV (141a) |  -5.547 eV (141a) |
| Ph ₃ C≡CAu ₁₀ |  -5.474 eV (161a) |  -5.474 eV (161a) |

Table S4. Orbital energies (eV) and shapes of the high-lying S lone pair MOs for the Au/SPh_n Series.

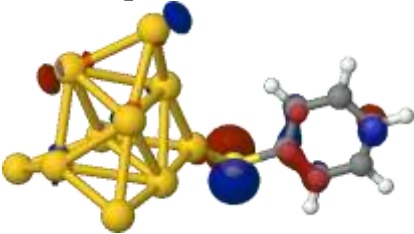
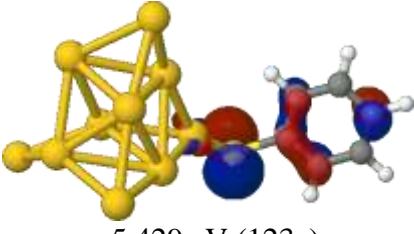
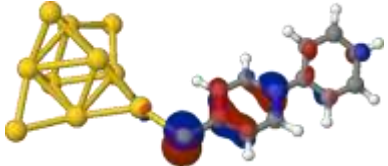
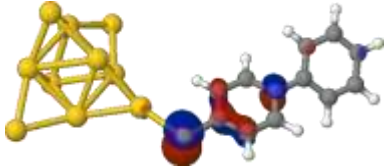
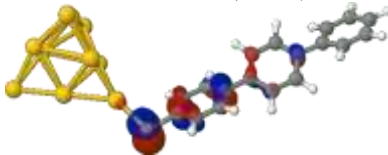
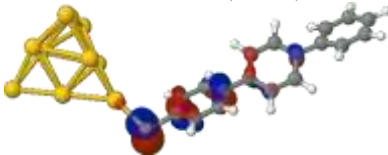
| Cluster | MO, S alpha | MO, S beta |
|-----------------------------------|---|---|
| PhSAu ₁₀ |  -5.532 eV (123a) |  -5.429 eV (123a) |
| Ph ₂ SAu ₁₀ |  -5.714 eV (143a) |  -5.279 eV (143a) |
| Ph ₃ SAu ₁₀ |  -5.323 eV (163a) |  -5.325 eV (163a) |

Table S5. Orbital energies (eV) and shapes of the S lone pair MOs using $\text{Ph}_n\text{CH}_2\text{SAu}_{10}$ closed-shell cluster models for the Ag/SCH₂Ph_n Series.

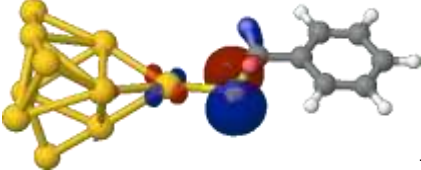
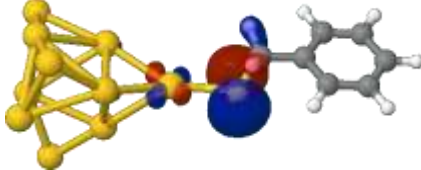
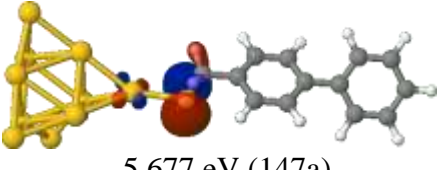
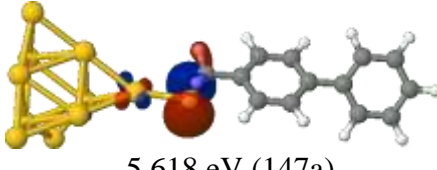
| Cluster | MO, S alpha | MO, S beta |
|---|---|--|
| $\text{PhCH}_2\text{SAu}_{10}$ |  5.640 eV (127a) |  5.598 eV (147a) |
| $\text{Ph}_2\text{CH}_2\text{SAu}_{10}$ |  -5.677 eV (147a) |  -5.618 eV (147a) |

Table S6. Orbital energies (eV) and shapes of the S lone pair MOs using $\text{Ph}_n\text{CH}_2\text{SAg}_9$ closed-shell cluster models for the Ag/SCH₂Ph_n Series.

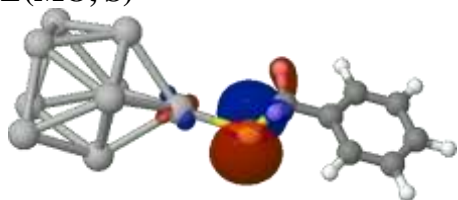
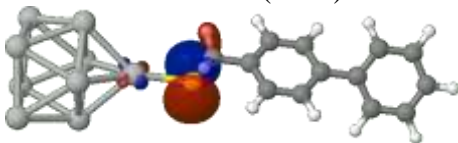
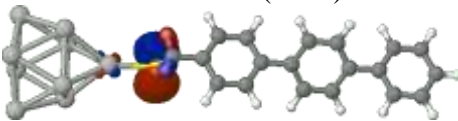
| Cluster | $E(\text{MO}, \text{S})$ |
|--------------------------------------|---|
| $\text{PhCH}_2\text{SAg}_9$ |  -4.981 eV (118a) |
| $\text{Ph}_2\text{CH}_2\text{SAg}_9$ |  -5.009 eV (138a) |
| $\text{Ph}_3\text{CH}_2\text{SAg}_9$ |  -5.020 eV (158a) |

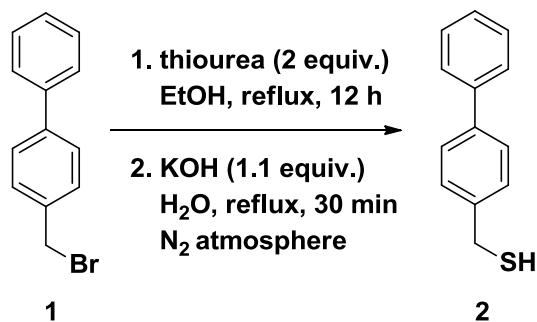
Table S7. HOMO energies and HOMO–LUMO gaps of aromatic molecules in vacuum. The computational approach is identical to that used for the molecule–metal complexes.

| Molecule | <i>E</i>(HOMO), eV | <i>E</i>(gap), eV |
|--------------------|---------------------------|--------------------------|
| PhSH | −5.914 | 5.594 |
| Ph ₂ SH | −5.716 | 4.765 |
| Ph ₃ SH | −5.631 | 4.357 |

| Molecule | <i>E</i>(HOMO), eV | <i>E</i>(gap), eV |
|------------------------------------|---------------------------|--------------------------|
| PhCH ₂ SH | −6.225 | 5.750 |
| Ph ₂ CH ₂ SH | −6.061 | 5.010 |
| Ph ₃ CH ₂ SH | −5.883 | 4.551 |

| Molecule | <i>E</i>(HOMO), eV | <i>E</i>(gap), eV |
|----------------------|---------------------------|--------------------------|
| PhC≡CH | −6.466 | 5.449 |
| Ph ₂ C≡CH | −6.094 | 4.696 |
| Ph ₃ C≡CH | −5.897 | 4.335 |

Synthesis of $\text{HSCH}_2(\text{C}_6\text{H}_4)_2$ ((1,1'-biphenyl)-4-ylmethanethiol). We followed a previously reported literature procedure.¹⁴ A 25 mL ethanolic solution containing 4-(bromomethyl)-1,1'-biphenyl (**1**) (4 mmol) and thiourea (608 mg, 8 mmol) was heated under reflux condition for 12 h (Scheme S1). After being cooled to room temperature, the reaction solvent was removed *in vacuo*, followed by addition of aqueous solution of KOH (246 mg, 4.4 mmol in 20 mL degassed water). The reaction mixture was again heated under reflux for 30 min under a N_2 atmosphere (Note: longer reaction time may cause oxidation of the thiol group). The reaction solution was cooled to room temperature, and extracted with cold ($T = 0^\circ\text{C}$) CH_2Cl_2 . The combined organic layer was dried over anhydrous MgSO_4 , filtered to remove suspended solid, and concentrated *in vacuo* (Note: the temperature of water bath must be below 30°C) to yield a white solid product. $\text{Mp} = 77\text{--}78^\circ\text{C}$; $^1\text{H NMR}$ (CDCl_3) δ 1.80 (t, $J = 8.0$ Hz, 1H), 3.79 (d, $J = 8.0$ Hz, 2H), 7.32-7.46 (m, 5H), 7.54-7.59 (m, 4H); $^{13}\text{C NMR}$ (CDCl_3) δ 28.9, 127.3, 127.5, 127.7, 128.7, 129.0, 140.3, 140.4, 141.0.¹⁵



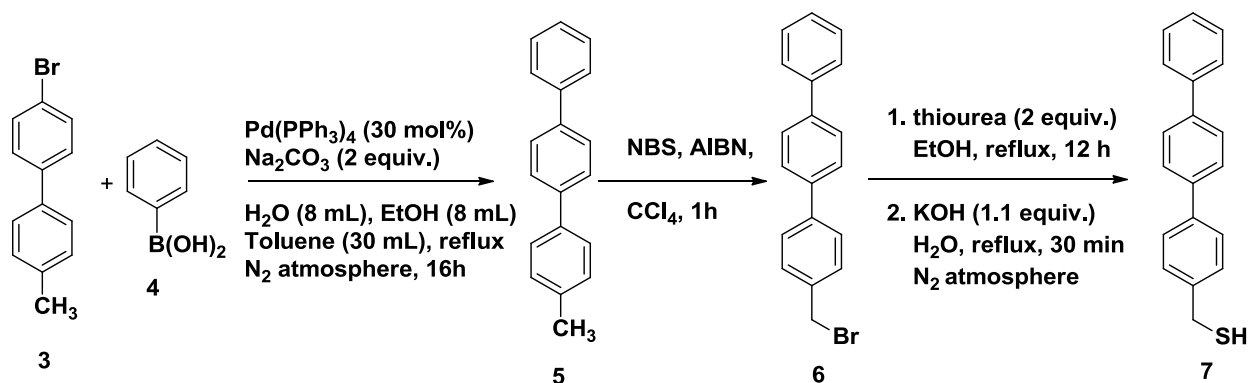
Scheme S1. Synthesis of [1,1'-biphenyl]-4-ylmethanethiol

Synthesis of $\text{HSCH}_2(\text{C}_6\text{H}_4)_3$ (4-methyl-1,1':4',1''-terphenyl). A degassed mixture of Na_2CO_3 (2.2 g, 21 mmol), tris(4-methylphenyl)boroxin (1.3 g, 3.7 mmol), $\text{Pd}(\text{PPh}_3)_4$ (0.35 g, 0.30

mmol), 4-bromo-4'-methyl-1,1'-biphenyl (**3**) (2.47 g, 10 mmol), H₂O (8 mL), EtOH (8 mL), and toluene (30 mL) was stirred under N₂ at 80 °C for 16 h (Scheme S2). After cooling, the aqueous layer was removed and the organic phase was evaporated to dryness. Chromatography on silica (CH₂Cl₂) yielded a reddish solid, which was recrystallized from cyclohexane to give colorless solid. ¹H NMR (CDCl₃): 2.43 (s, 3 H, CH₃), 7.29 (d, *J* = 8 Hz, 2H, ArH), 7.36-7.40 (m, 1H, ArH), 7.48 (t, *J* = 8 Hz, 2H, ArH), 7.57 (d, *J* = 8 Hz, 2H, ArH), 7.66-7.69 (m, 6H, ArH). ¹³C (CDCl₃): 21.1, 126.9, 127.0, 127.3, 127.5, 128.8, 129.5, 137.1, 137.8, 139.8, 140.0, 140.7.

Synthesis of 4-(bromomethyl)-1,1':4',1''-terphenyl (6). **5** (0.5 g, 2 mmol), NBS (0.4 g, 2.2 mmol) and 20 mg of AIBN were heated to reflux in CCl₄ for 1 h. After 30 min, some more AIBN (20 mg) was added to the mixture. Removal of the solvent, followed by filtration through a pad of silica (using CH₂Cl₂ as a solvent) yielded a white solid (0.63 g, 95%) (Scheme S2). The product was used without any purification in the next step. ¹H NMR: 4.57 (s, 2H, CH₂Br), 7.38 (d, *J* = 8 Hz, 1H, ArH), 7.44-7.50 (m, 4H, ArH), 7.61-7.69 (m, 8H, ArH).

Synthesis of [1,1':4',1''-terphenyl]-4-ylmethanethiol (7). Following the same procedure described for **2**, we synthesized **7** in 80% overall yield (Scheme S2). M.p. 205 – 207 °C. ¹H NMR (CDCl₃): 1.82 (t, *J* = 7.7 Hz, 1 H, SH), 3.81 (d, *J* = 7.6 Hz, 2 H, ArCH₂S), 7.35 - 7.49 (m, 5 H), 7.57 - 7.67 (m, 8 H). ¹³C (CDCl₃): 28.7, 127.0, 127.3, 127.4, 127.5, 128.5, 128.8, 139.5, 139.6, 140.2, 140.3, 140.7.



Scheme S2. Synthesis of [1,1':4',1''-terphenyl]-4-ylmethanethiol (**7**)¹⁶

Synthesis of 4-Ethynyl-p-terphenyl. We followed the procedure described in reference 17.¹⁷ ¹H

NMR (CDCl₃) δ 3.14 (s, 1H), 7.37–7.58 (m, 3H), 7.59–7.69 (m, 10H).

REFERENCES

- (1) Weiss, E. A.; Kaufman, G. K.; Kriebel, J. K.; Li, Z.; Schalek, R.; Whitesides, G. M. *Langmuir* **2007**, *23*, 9686-9694.
- (2) McDonagh, A. M.; Zareie, H. M.; Ford, M. J.; Barton, C. S.; Ginic-Markovic, M.; Matisons, J. G. *J. Am. Chem. Soc.* **2007**, *129*, 3533-3538.
- (3) Zaba, T.; Noworolska, A.; Bowers, C. M.; Breiten, B.; Whitesides, G. M.; Cyganik, P. *J. Am. Chem. Soc.* **2014**, *136*, 11918-11921.
- (4) Bowers, C. M.; Liao, K.-C.; Yoon, H. J.; Rappoport, D.; Baghbanzadeh, M.; Simeone, F. C.; Whitesides, G. M. *Nano Lett.* **2014**, *14*, 3521-3526.
- (5) de Boer, B.; Meng, H.; Perepichka, D. F.; Zheng, J.; Frank, M. M.; Chabal, Y. J.; Bao, Z. N. *Langmuir* **2003**, *19*, 4272-4284.
- (6) Shaporenko, A.; Cyganik, P.; Buck, M.; Terfort, A.; Zharnikov, M. *J. Phys. Chem. B* **2005**, *109*, 13630-13638.
- (7) Tao, Y. T.; Wu, C. C.; Eu, J. Y.; Lin, W. L.; Wu, K. C.; Chen, C. H. *Langmuir* **1997**, *13*, 4018-4023.
- (8) Becke, A. D. *J. Chem. Phys.* **1993**, *98*, 5648-5652.
- (9) Eichkorn, K.; Treutler, O.; Ohm, H.; Haser, M.; Ahlrichs, R. *Chem. Phys. Lett.* **1995**, *242*, 652-660.
- (10) Weigend, F.; Ahlrichs, R. *Phys. Chem. Chem. Phys.* **2005**, *7*, 3297-3305.
- (11) Weigend, F. *Phys. Chem. Chem. Phys.* **2006**, *8*, 1057-1065.
- (12) Andrae, D.; Haussermann, U.; Dolg, M.; Stoll, H.; Preuss, H. *Theor. Chim. Acta* **1990**, *77*, 123-141.
- (13) Furche, F.; Ahlrichs, R.; Hattig, C.; Klopper, W.; Sierka, M.; Weigend, F. *Wires Comput. Mol. Sci.* **2014**, *4*, 91-100.

- (14) Yoon, H. J.; Bowers, C. M.; Baghbanzadeh, M.; Whitesides, G. M. *J. Am. Chem. Soc.* **2014**, *136*, 16-19.
- (15) Kadjout, M.; Hebling, Y.; Albrecht, P.; Adam, P. *Chem. Biodivers.* **2012**, *9*, 714-726.
- (15) Himmel, H. J.; Terfort, A.; Woil, C. *J. Am. Chem. Soc.* **1998**, *120*, 12069-12074.
- (16) Shakirova, J. R.; Grachova, E. V.; Melekhova, A. A.; Krupenya, D. V.; Gurzhiy, V. V.; Karttunen, A. J.; Koshevoy, I. O.; Melnikov, A. S.; Tunik, S. P. *Eur. J. Inorg. Chem.* **2012**, 4048-4056.